# Semiconductor Nanomembrane Tubes: Three-Dimensional Confinement for Controlled Neurite Outgrowth

**Minrui Yu,[†,∥,*] Yu Huang,[‡,∥,*] Jason Ballweg,[§] Hyuncheol Shin,[†] Minghuang Huang,[⊥] Donald E. Savage,[⊥] Max G. Lagally,[⊥] Erik W. Dent,[§] Robert H. Blick,[†] and Justin C. Williams[‡,*]**

[†]Department of Electrical and Computer Engineering, [‡]Department of Biomedical Engineering, [§]Department of Anatomy, and [⊥]Department of Materials Science and Engineering, University of Wisconsin—Madison, Madison, Wisconsin 53706, United States. [∥] These authors contributed equally to this work.

**ABSTRACT** In many neural culture studies, neurite migration on a flat, open surface does not reflect the three-dimensional (3D) microenvironment *in vivo*. With that in mind, we fabricated arrays of semiconductor tubes using strained silicon (Si) and germanium (Ge) nanomembranes and employed them as a cell culture substrate for primary cortical neurons. Our experiments show that the SiGe substrate and the tube fabrication process are biologically viable for neuron cells. We also observe that neurons are attracted by the tube topography, even in the absence of adhesion factors, and can be guided to pass through the tubes during outgrowth. Coupled with selective seeding of individual neurons close to the tube opening, growth within a tube can be limited to a single axon. Furthermore, the tube feature resembles the natural myelin, both physically and electrically, and it is possible to control the tube diameter to be close to that of an axon, providing a confined 3D contact with the axon membrane and potentially insulating it from the extracellular solution.

**KEYWORDS:** semiconductor nanomembrane tubes · neuron—semiconductor interface · guided neuron outgrowth · neuronal network · 3D scaffold · myelin sheath

Brains and computers are alike in the sense that both rely on a network of billions of basic operating units, either neurons or transistors, to function properly, and both use electrical signals to transmit information. Not surprisingly, researchers have been trying to combine them to make hybrid neural electronic systems,[1,2] such as brain—computer interfaces (BCI),[3] motor prosthetic devices,[4] and deep brain stimulation (DBS).[5] Such endeavors will benefit from *in vitro* studies for a better understanding of the interface between organic neurons and inorganic electronics. A neural culture platform should take the following into consideration: First, transmembrane currents and the resulting voltage potentials from neurons are very weak, falling off quickly from the cell body, and are subject to background noise.[6,7] Consequently, interfacing electrodes need to be in close proximity to the neuron cell body or its processes. They also have to be sufficiently small, often on the order of an individual cell body, to isolate signals from a single neuron while not picking up the activity of nearby cells. Second, *in vitro* study of neuron activity favors the establishment of a one-to-one electrode—neuron correspondence. Hence it is desirable to arrange neuron outgrowth into a defined network, where synaptic contacts can be controlled spatially. Third, neurons have the capability to alter their responses to local surroundings dramatically.[8] Ideal cultures should therefore mimic the native neural microenvironment to capture the normal cell behavior.

Advances in micro/nanofabrication have enabled us to make ever smaller devices with increasingly higher spatial resolution, as demonstrated by the use of complementary metal-oxide semiconductor (CMOS) chips and nanowire field effect transistors (FETs) to interface with neurons.[9,10] A variety of approaches has also been presented to guide neuron outgrowth, including chemical tracks,[11,12] picket fences,[13] 3D cages,[14] and microgrooves.[15] Largely ignored, however, is the behavior *versus* environment aspect, with most *in vitro* studies having their neural processes (neurites) migrate on a flat surface and cells directly exposed to the culture solution. In contrast, *in vivo* conditions are 3D by nature, and many axons are ensheathed in glial cell membranes (myelin).[16,17] The myelin sheath is a dielectric layer that wraps around the axon. It leads to salutatory conduction by eliminating the loss of ions through the leakage channels and increasing the distance between the action potential generation

* Address correspondence to myu3@wisc.edu, yuhuang@wisc.edu, jwilliams@engr.wisc.edu.

Received for review December 29, 2010 and accepted March 2, 2011.

**Published online March 02, 2011**
**10.1021/nn103618d**

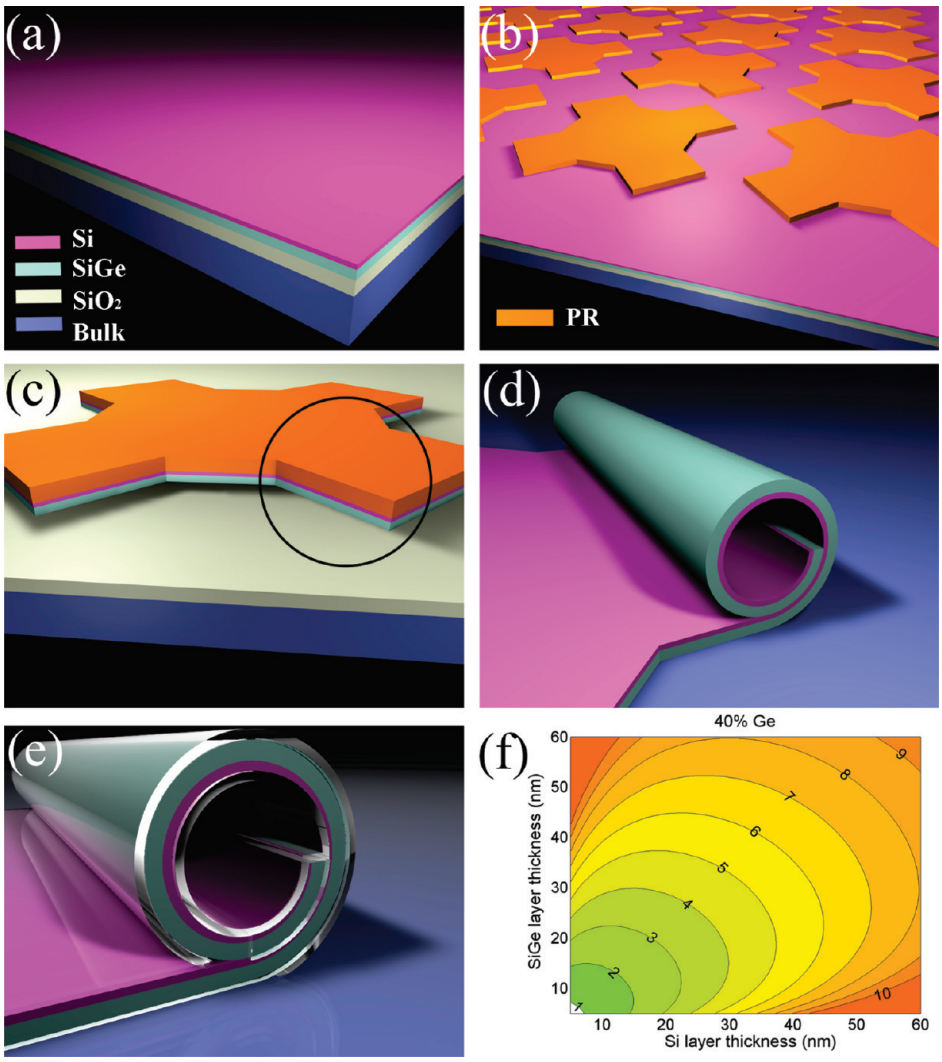


**Figure 1. Fabrication diagrams and contour plots of tube diameters. (a) Initial material, with Si epitaxially grown on SGOI; (b) arrays patterned by lithography, using photoresist (PR) as an etch-stop for the next step; (c) with a single pattern as an example, reactive-ion etching (RIE) to define the mesa (note $SiO_2$ survives this step because it has a very low etch rate); (d) after HF etching, the circled part from step (c) rolls up into a tube; (e) optional coating with biocompatible polymer to passivate the surface; (f) contour plot of how Si and SiGe layer thicknesses affect the tube diameter, at 40% Ge concentration in the SiGe alloy. The values on the contours are tube diameters in micrometers.**

nodes,[18] resulting in faster signal propagation along myelinated axons than unmyelinated ones.

In this work, we demonstrate the growth of neurites through arrays of semiconductor nanomembrane tubes. The three-dimensional (3D) topography of the tube not only can promote neuron outgrowth but also has potential to isolate the neurites from the bulk extracellular solution. Furthermore, the tubular structure makes it possible to implement the so-called "cuff electrode" design that has been widely utilized for electrical coupling in *in vivo* isolated nerve preparations.[19]

## RESULTS AND DISCUSSION

Our tubes are made of silicon (Si) and silicon–germanium (SiGe) bilayer nanomembranes with Si epitaxially grown on $Si_{0.8}Ge_{0.2}$, which is the top layer of SiGe-on-insulator (SGOI, Soitec, Inc.). The SGOI consists of 30 nm of SiGe, 190 nm of silicon dioxide ($SiO_2$) as a differentially etchable release layer, and a Si substrate (handle wafer). Because Si and Ge have different lattice constants, there exists a strain gradient, with the epitaxial Si tensilely strained to match the lattice constant of SiGe. When the sacrificial oxide layer is removed by hydrofluoric (HF) acid, the Si/SiGe bilayer shares strain by rolling up, a mechanism called "lattice misfit induced self rolling".[20−22] The strain that causes the rolling and hence the curvature of the tube can be precisely controlled by material properties, as follows:[23]

$$\frac{1}{R} = 6x\frac{\Delta a}{a}\frac{t_{Si}t_{SiGe}}{(t_{Si}+t_{SiGe})^3} \quad (1)$$

where $x$ is the Ge concentration in the $Si_{1-x}Ge_x$ alloy, $\Delta a/a$ is the lattice mismatch ratio, and $t_{Si}$ and $t_{SiGe}$ are

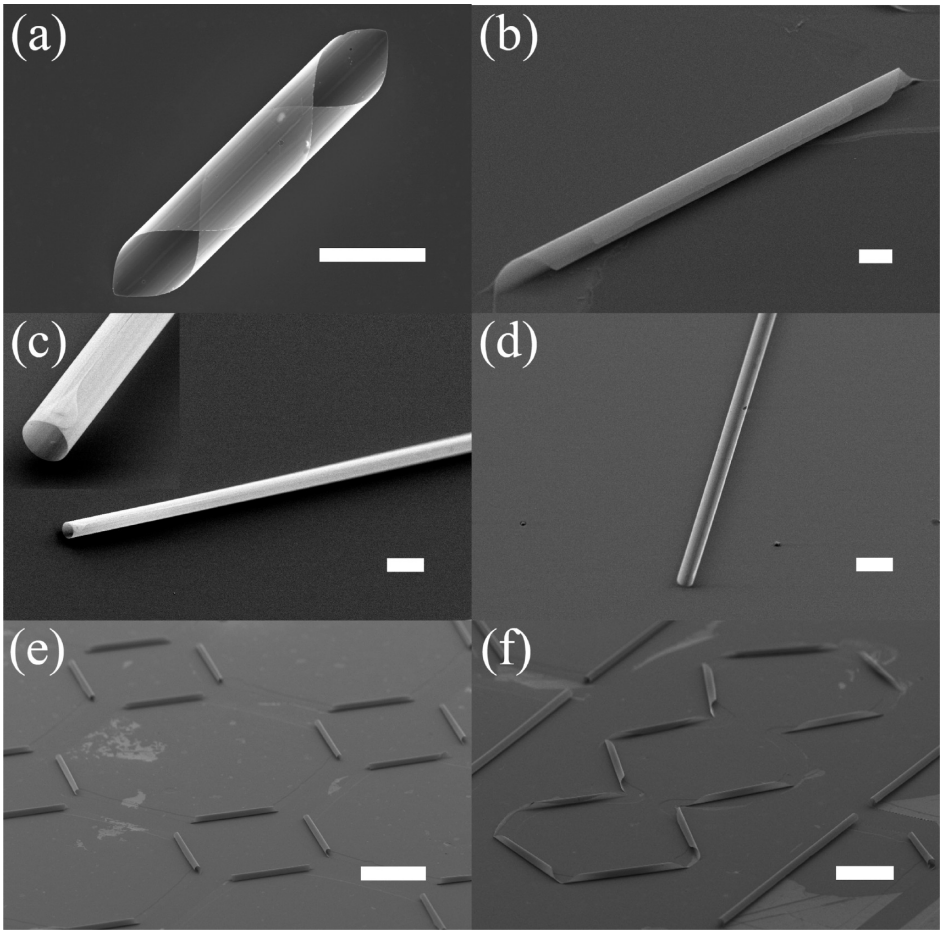


**Figure 2. Three-dimensional rolled-up structures: (a) cannoli-shaped tube; (b) multiwalled tube; (c) long single-walled tube, with inset showing a close-up view; (d) open half-tube; (e) square tube arrays; (f) zigzag network. Scale bar is 100 $\mu$m for (e) and (f) and 10 $\mu$m for all others.**

the thicknesses of the Si and SiGe layers, respectively. For recent reviews on semiconductor nanomembranes, see refs 24 and 25.

Figure 1a−e schematically describes the fabrication process. We start with the epitaxial growth of Si on top of a SGOI wafer. Optical or electron-beam lithography is used to define the patterns. The remaining photoresist (PR) after development serves as an etch-stop for reactive-ion etching (RIE), which removes the materials surrounding the regions that become the tubes and expose the sacrificial layer underneath. Subsequent HF etching releases the strained Si/SiGe bilayer, causing it to roll up into tubes. As an optional step, polymers can be coated on the sample surface to make it entirely biocompatible (this step will be further discussed later). Figure 1f is a contour plot calculated from eq 1. It shows the predicted tube diameters as a function of the thicknesses of the Si and SiGe layers, with 40% Ge in the SiGe alloy. It is clear that, for a given Ge concentration, we can have continuous coverage of tube diameters over a range that is relevant to neuronal cell culture applications. This gives us a choice of potential diameters, which may be important as *in vivo* nerves exhibit variability in axon diameter between different species, between different anatomical areas, and even within individual nerve bundles.[26] In the majority of the experiments presented here, the tube diameter was 8.2 $\mu$m, but we also made some measurements with 4 $\mu$m tube diameters.

The flexibility of this fabrication technique allows us to make tubes with distinctive features. With careful pattern designs and alignment along particular crystallographic directions, we can have taper-ended tubes (Figure 2a,b) or blunt-ended tubes (Figure 2c,d). Controlling the pattern size and etching time will provide multiwalled tubes (Figure 2a,b), single-walled tubes (Figure 2c), or open tubes (Figure 2d). It is even possible to adjust the curvature with pattern designs. For example, Figure 2c shows a tube with half the diameter one would normally get. All of these features can be parallel processed and arranged into networks, such as those in Figure 2e,f. It is also worthwhile to note that the tube length is only dependent on the pattern design and can be adjusted to hundreds of micrometers or more, lengths that are typical for myelinated segments of axons.[27]

In order to use the tube-containing substrate in cell culture applications, it is necessary first to validate that

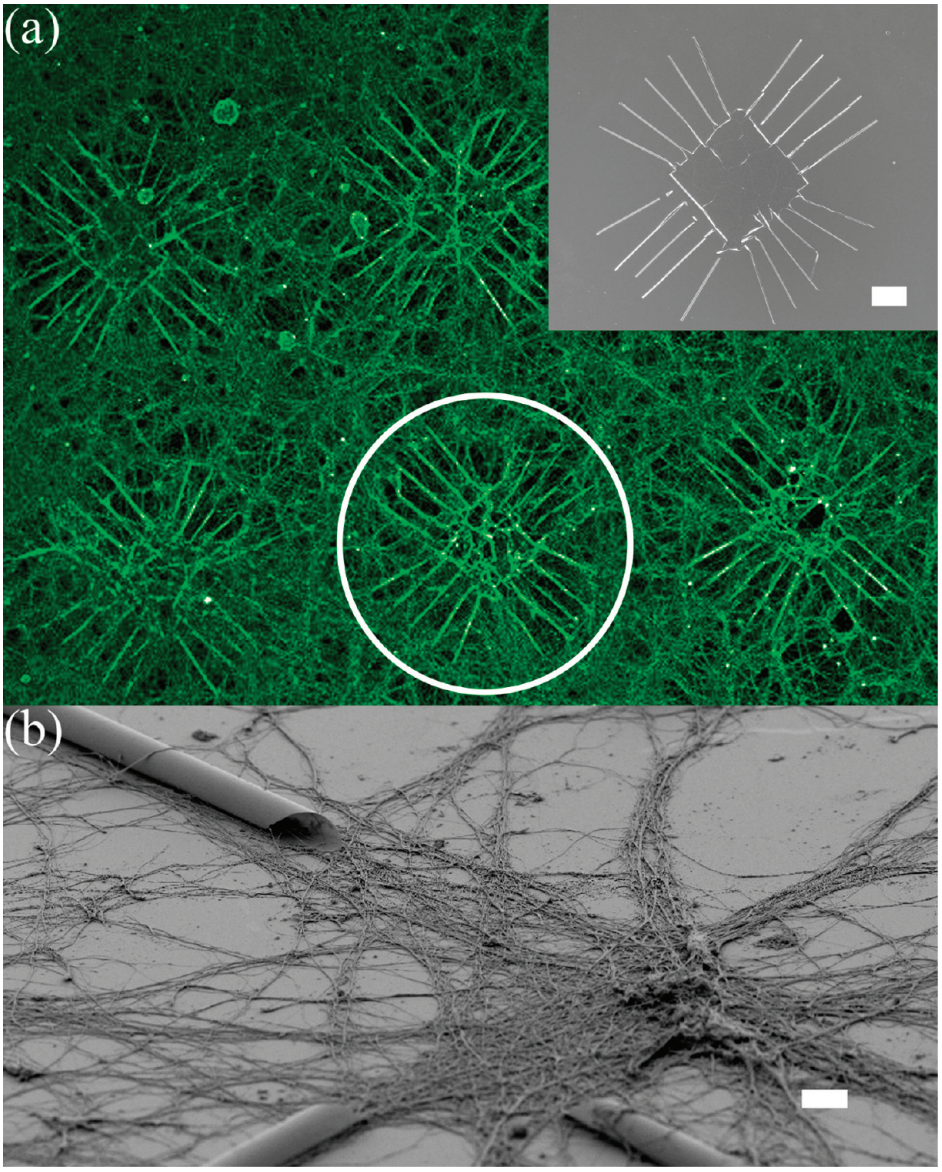


**Figure 3. Fluorescent microscopy and SEM images of cortical neurons cultured on a Si wafer with Si/SiGe tubes. (a) Pseudocolored fluorescent image of neurons growing extensively on an array of patterns, which consist of multiple extending tubes on each side. Inset is a SEM picture of the pattern. The fluorescent image, is taken using antibody to tubulin that heavily labels dendrites and axons. Semiconductor structures are invisible in the fluorescent image, but are outlined by the contrast of surrounding fluorescently labeled neurons and processes, as shown inside the white circle. (b) SEM image of neurons at an intersection of several tubes. Neurons appear to grow processes in the entire area, although more concentrated in the vicinity of the tubes. Scale bar is 100 $\mu$m for (a) and 10 $\mu$m for (b).**

the material is nontoxic. Although Si and other semiconductors have been shown to be capable of supporting cellular growth,[28,29] SiGe has not been reported as a viable cell culture substrate. We tested the platform's viability for *in vitro* neural cultures using E15.5 cortical neurons obtained from Swiss Webster mice, a commonly used neural cell culture model. A brief description of the culture procedure is given in the Methods section, and full details can be found elsewhere.[30,31] Fluorescent imaging of live and fixed samples and scanning electron microscope (SEM) imaging were performed after 7 days. In all of the samples we investigated, the neural cells showed normal morphology and neurite extension for cultures of this type and age (Figure 3). Neurons were able to grow on both SiGe and Si surfaces. The images compare favorably to studies reported elsewhere.[32] This observation is not necessarily surprising, as the earlier experiments by others also involved substrates that were covered completely with poly-D-lysine (PDL), a highly positively charged synthetic amino acid chain that is commonly used as a coating to promote cell adhesion. This result does suggest the ability of the substrate to support *in vitro* neural culture, and the substantial growth of neurites into tubes further substantiates that those surfaces are not toxic to the cells, as the closed volume

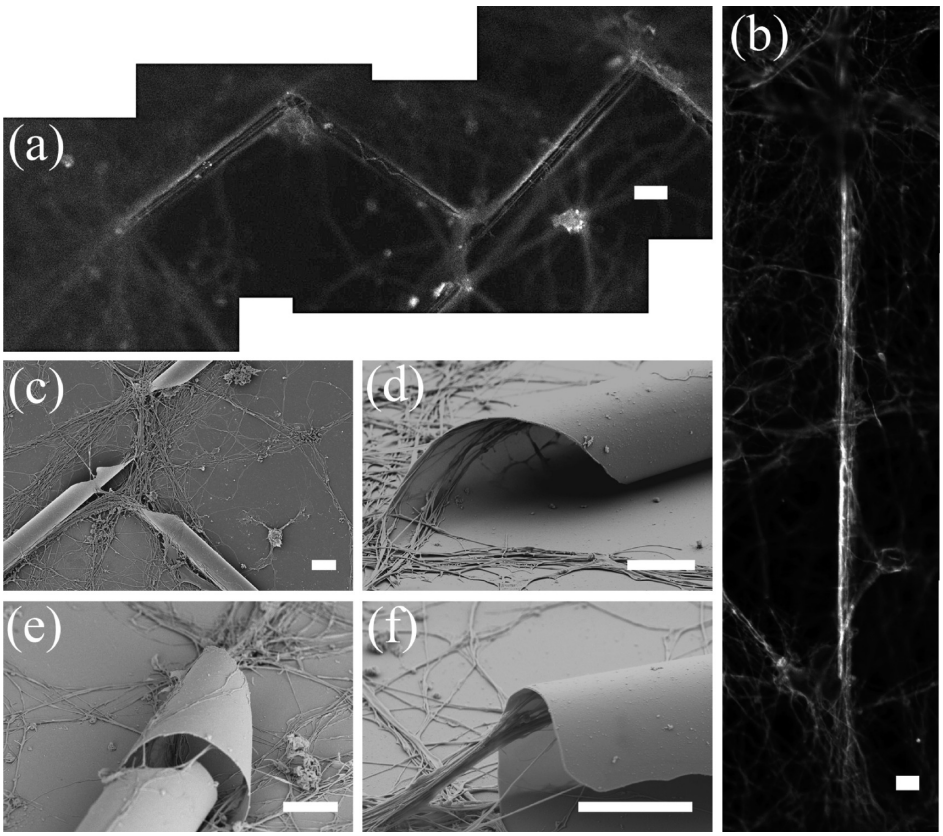


**Figure 4. Growth patterns of neurons with tubes: fluorescent images of (a) neurites growing along a zigzag tube network, and (b) a neurite, potentially a single axon, growing in a 4 $\mu$m diameter tube. Corresponding SEM images of the tubes in (a) and (b) are shown in Figure 2f and 2c, respectively; (c) neurons tend to grow by following the tube structure, some even into the tubes; (d) for taper-ended tubes, neurites grow inside the tubes in a helical fashion, following the configuration of the tube rolling edge; (e) neurites growing on the outside surface of a tube. Neurites inside the tube are shown through a nick in the tube; (f) neurites stretch out at the end of a blunt-ended tube. Note neurites tend to attach to the top wall inside the tube. Scale bar is 20 $\mu$m for (a) and (b) and 5 $\mu$m for all others.**

of the inside of the tubes would accumulate any toxic factors and likely lead to increased neural degeneration. In order to determine if the tube geometry alone (without adhesion molecules) is sufficient to attract neurite outgrowth, we further investigated the ability of the substrate to support neural growth by selectively patterning small islands of PDL near the entrance of the tubes, leaving all other areas uncoated. The results are shown later in this paper.

We want to point out that the use of quantitative assessments in this application, such as counting process numbers, neurite growth rates, and time to development of major axons, would be confounded by the presence of the tubes. Further study is needed to associate these various assessments with the tube size, cross section geometry, internal features of the tube walls, density of tubes on the surface, *etc*. However, none of these assessments would change our basic finding that the substrate is not toxic and can support neural growth.

Three-dimensional nanomembrane geometry has been shown to influence cell growth[33,34] and is an emerging area of investigation across a variety of *in vitro* culture applications. Our cell culture results build upon these recent studies and indicate that neurons also appear to be attracted to grow in or along the tubular structures. We observed increased neural extension near the tubes, indicating that such micrometer-sized confinement may be preferential for neuron outgrowth. Several growth patterns can occur: neurites can grow outside the tube and along the tube edge (Figure 4a,c), or they can grow on top of the tube and follow the curved surface (Figure 4e); more interestingly, they can grow inside and through the tube. Figure 4a provides a good overview of all of these features: due to light refraction, images of neural extensions along the outer edge of the tubes are blurred, but they help to identify the profile of the tubes; the curly lines along the tube in the middle are neurites growing on the convex outer surface of the tube, and the straight lines along the left and right tubes are neurites growing inside the tubes. The inside growth is evidenced by their slightly fainter appearance. Further, in the case when neurites grow into the tube, there are also variations depending on the tube configuration. For example, for taper-ended tubes, they can grow into 3D helices by following the tube rolling trend (Figure 4d), while for blunt-ended tubes,

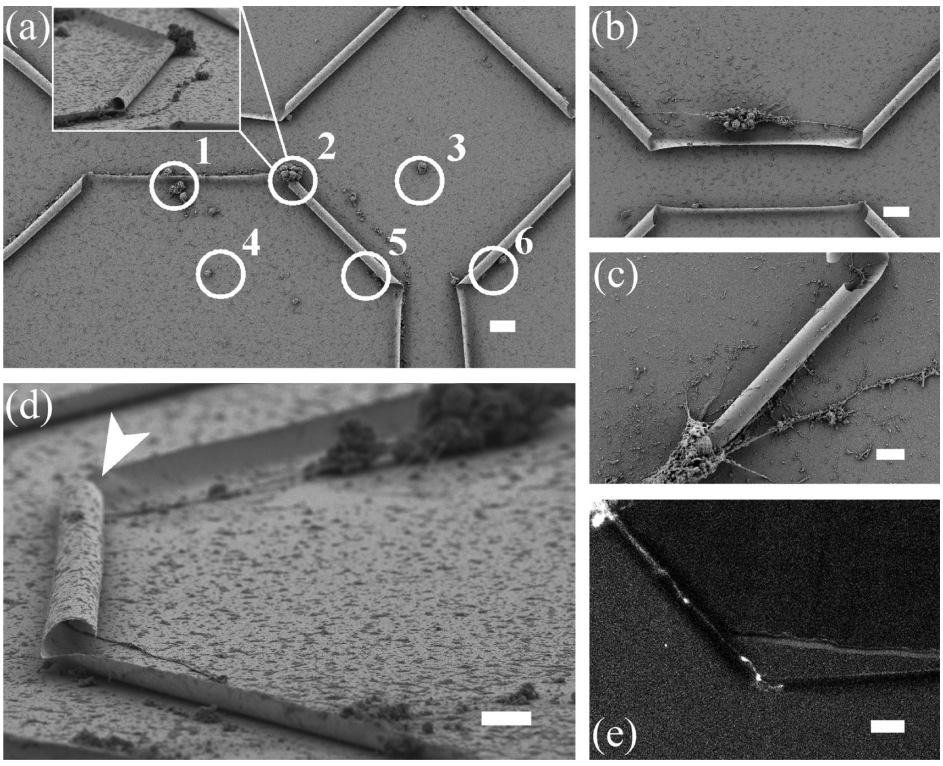


**Figure 5. PDL printing for single-neurite growth through semiconductor tubes. (a) Neurons are shown to adhere to printed PDL dots (white circles): dots near curved surfaces (1 and 2) seem to have better cell adhesion and development than dots on flat surfaces (3 and 4). In addition, cells at printed PDL dots that are far from 3D features do not send out any processes (3 and 4). Inset is an angled view of dot 2, where neurites growing into the tube could completely fill the entrance; (b) a neural aggregate positioned between two tubes is seen here to send out primary processes directly to the two tubes; (c) extending processes cause neuronal soma migration that completely fills the entrance of a tube; (d) a single axon grows in (shown by arrow) and out of the other side of an 80 $\mu$m long tube; (e) snapshot from a fluorescent time-lapse sequence showing a single axon growing through a tube (confirmed by subsequent SEM image). The axonal growth cone can be seen at the leading edge of the axon in the middle of the image. Scale bar is 10 $\mu$m for (c) and (d) and 20 $\mu$m for all others.**

they can extend into a straight line inside the tube (Figure 4b), even stretching and becoming suspended at the tube end (Figure 4f). A possible explanation of this behavior is that, for 3D topographical surfaces with a gradual transition, such as the case for taper-ended tubes rolling off a plane, extending processes tend to maintain their original growth direction and end up with a spiral pattern. Conversely, for surfaces with abrupt changes, such as that involving a blunt-ended tube and the substrate, they will try to pull between the contact points on the two surfaces. A similar phenomenon has been observed for neurites bridging across micropatterned grooves.[35] In these previous studies, the angle of incidence between the developing neurite and the groove wall was found to be important in determining the growth of the neurite up the groove wall. This could also be true in our case as neurites encounter the entrance geometry of the tubes.

It should be noted that sample preparation steps for SEM imagining are known to cause tissue shrinkage.[36] In our experiment, shrinkage of the neural processes is significant: the imaged diameter lies between 60 and 840 nm, in contrast to a normal diameter of 2−3 $\mu$m for *in vivo* axons, for example. In addition, because the tube size is larger than a single axon, it is likely that multiple processes can pass through it, as indicated by the bundle of neurites in Figure 4d,f. Thus, several neural processes appear to grow through the tube, either simultaneously or in a staggered fashion, and may even completely fill the inside volume of the tube. This structure may be similar to a bundle of small-caliber axons that are ensheathed by a single glial cell membrane, which is known to occur *in vivo*.

Nevertheless, a more interesting scenario is to have the tube size close to that of an axon so that only one is allowed to grow inside. An initial attempt was made to fabricate tubes with 4 $\mu$m diameter (Figure 2c). As shown in Figure 4b, fluorescent imaging indicated neurites can still grow into tubes of this size (we can tell the neurite is inside because it has a clear edge toward the tube wall, indicating contact, but not so toward the middle of the tube). Given the diameter and the length of the tube, most likely the neurite was a single axon. While it appears that the tube size in Figure 4b can be further decreased, it may not be crucial to match the exact *in vivo* nerve diameter, as axons change their diameter throughout development and even during regrowth. For example, there is

supporting evidence that regenerating neurons can accommodate the size of their surroundings and dynamically change their shape in the presence of external pressure.[37] This behavior suggests that achieving a nominal diameter may be sufficient and the developing axon would adjust its size to fit the tube. More extensive work is currently underway to investigate the tube size range that is most effective for neural guidance and coupling.

Figures 3 and 4 show that seeding neurons without discretion leads to neurite outgrowth on the entire substrate surface, which is coated with PDL. What effects does the Si/SiGe substrate, and particularly the tubular geometry alone, have on neural growth? In order to answer this question, we employed an inkjet printing technique (DMP-2800 series Diamatix Materials Printer, FUJIFILM) that allows us to deposit small areas of PDL both near the entrance to individual or groups of tubes as well as in areas far away from the tubes (Figure 5a). Such an inkjet process is necessary because it is noncontact and does not risk damaging the tube structures as other patterning techniques, such as microcontact printing, might. PDL dots near 3D features (1 and 2 in Figure 5a) seem to have better cell adhesion and development than those on a flat, open surface (3 and 4 in Figure 5a). To increase the chances of guided neuron outgrowth, it is desirable to put neurons near the ends of a tube. Figure 5b shows that when a neural aggregate is positioned between two tubes and within a critical range (roughly less than 70 $\mu$m), the primary processes are sent directly toward the two tubes. Clearly, neurites are able to grow on the areas of the sample surfaces not coated with PDL, reconfirming our earlier finding that Si/SiGe is a viable material for neural culture. It is interesting, however, that the neurites prefer to grow into the tube, even without any adhesion promoter inside. The same cannot be said for the native, planar Si surfaces, where neurite extension is limited. This finding agrees with previous results of PDL dots on gold that are surrounded by a cell repulsive background.[38] In an effort to seed a single neuron, we have controlled the diameter of printed PDL to be as small as 15 $\mu$m. Figure 5c shows that the somata, potentially migrating toward the tube or even mechanically tensioned by neurite outgrowth through the tube, can completely block the tube entrance. Figure 5d is a SEM image showing a neurite not only passing through a tube but also turning itself before and after the tube to follow the topography. Figure 5e is a snapshot from a movie recording a neurite exiting the tube on the left and beginning to enter the tube on the right. Further time lapse microscopy experiments will be instrumental in elucidating the mechanisms by which cells locate the tube entrance and position the soma relative to the tube inlet.

As with the material toxicity studies mentioned earlier, new quantitative measures will have to be developed to understand better how the presence of the tubes affects both growth rate and maturation. For example, it has become common to quantify differentiation/development by classifying neurons into developmental stages.[39] Using this assay, 100% of the neurons grown at the PDL spots patterned on the tube substrate had reached stage 5 of development by day 7, consistent with normal development. It is likely that they reached stages 3−5 earlier than normal, as the extension of the primary process was preferentially guided into the tube (Figure 5).

It has been reported that dendrites tend to retract after confined outgrowth over a distance of about 200 $\mu$m, whereas axons can remain straight and do not branch for more than 450 $\mu$m.[15] This phenomenon has been used in numerous recent microfluidic studies for "isolating" axons from soma and dendrites. Applied to our situation, in addition to controlling the tube diameter to be close to that of an axon (Figure 4b), we can further limit the outgrowth to be a single axon by guiding the neurite for a prolonged distance with a series of tubes (Figure 5c−e). Combining the ability to position neurons at specific locations with the precise mass production of tube arrays, we can guide neurite, and particularly axon, outgrowth and eventually even connect neurons into predetermined networks.

The 3D semiconductor nanomembrane not only has a unique structural advantage for neural cultures but also may provide some benefits in terms of electrical properties. An elongated neural fiber with a passive membrane can be modeled as a series of lumped RC circuits, where $r_m$ and $c_m$ are the unit length membrane resistance and capacitance, respectively.[40] It is well-known that a larger $r_m$ leads to reduced attenuation of the signal, while a smaller capacitance means faster signal propagation. For unmyelinated neocortical pyramidal axons, the specific resistance $r_m$ is 0.2 to 0.26 M$\Omega\cdot$cm and the specific capacitance $c_m$ is 0.63 to 1.25 nF/cm.[41] In comparison, for myelin sheath, these values are ~159 M$\Omega\cdot$cm and ~6.28 pF/cm, respectively.[27] Clearly, myelin increases the membrane resistance and decreases the capacitance. Considering the fact that successfully myelinating axons *in vitro* is challenging, many cell culture studies suffer from the large electrical property differences between myelinated and unmyelinated neurons. In this context, our tubes may fill such a gap by providing a dielectric insulation layer around growing neurites. With the current Si/SiGe material and taking into consideration the native oxide formed on the tube surfaces, the corresponding $r_m$ and $c_m$ are $3.92 \times 10^7$ M$\Omega\cdot$cm and 123 pF/cm, respectively. To increase the total tube resistance further and decrease its total capacitance, tubes with thicker walls, or multiwalled tubes like the one shown in Figure 2b, can be fabricated. However, the amount of strain in the material and the preference to match tube diameters to the axon size may limit our choices. A possible solution is to coat the sample

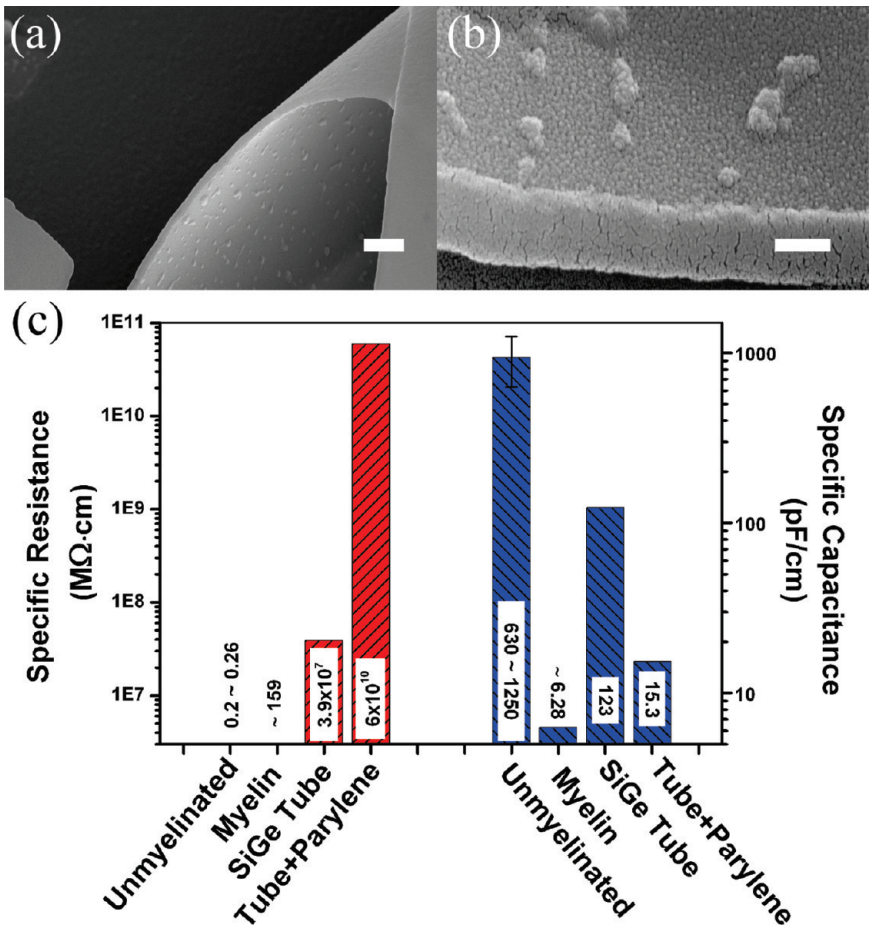


**Figure 6. SEM images of parylene-coated tubes and comparison of calculated electrical properties. (a) Parylene coating of the tube surface inside and out, (b) a closer look at the inner surface of the tube. The small bumps are regions of parylene condensation. The tube surfaces are completely covered by parylene as evidenced by the increase of the wall thickness from 50 nm to over 200 nm; (c) comparison of specific resistance and specific capacitance. Four cases are considered: unmyelinated axons, myelin sheath, and Si/SiGe tubes with and without parylene coating. Similar to myelin, the SiGe nanomembrane is able to increase the specific resistance and decrease the specific capacitance. Additional coating with parylene further enhances such effects. Scale bar is 1 $\mu$m in (a) and 200 nm in (b).**

surface with biocompatible polymers,[42] such as parylene-C (with volume resistivity $6 \times 10^{10}$ MΩ·cm and dielectric constant 3.15, Specialty Coating Systems). SEM images of parylene-coated tube surfaces are shown in Figure 6a,b. There are several advantages in this approach. First, parylene is well-known to be biocompatible. Second, parylene is coated in a chemical vapor deposition (CVD) process, which allows precise control of the deposited material thickness and thus fine-tuning of the electrical properties. Third, it is a conformal process so it can be done after the tube fabrication, without any interference with the geometry. A comparison of the electrical properties of unmyelinated axons and myelin sheath, as well as the properties of tubes with and without parylene coating, is shown in Figure 6c (assuming the parylene coating is 100 nm thick). It can be seen that the semiconductor tube potentially can act like myelin by increasing resistance and decreasing capacitance. Although it has a slightly larger specific capacitance than myelin, its specific resistance is several orders of magnitude higher. Adding a parylene layer further improves the situation and, with some tuning, it is possible to obtain resistance and capacitance that are comparable to (and possibly superior to) the natural myelin sheath.

Aside from parylene coating as an optional step of the tube fabrication process, metal contacts can also be made on the prerolled substrate (this will become the inner surface of the tube) before HF etching. After release, they will roll with the tubular structure into circular or spiral shapes,[43] making them perfect cuff electrodes. The cuff electrode technique has been used extensively in isolated nerve applications for gaining tight coupling of electrodes with nerve bundles for selective nerve stimulation and recording.[44,45] These devices can reduce the required stimulus current by an order of magnitude.[46] Considering the size of the tubes used in this study, it may be possible to make the equivalent of a "micro-cuff electrode" for a single axon.

Finally, the natural connections between glia and myelin make it tempting to introduce glia into the system. Neuron–glia mixed cultures have been

proposed for dissecting the complicated mechanisms behind implant failure and for high-throughput testing of new neuroelectrode designs.[47] Glia are also critical to the enhanced electrical activity in patterned cultures.[48] Although we have not deliberately excluded glia from our system, primary cultures at this age typically do not exhibit a noticeable glial population until much later. Prior work using polydimethylsiloxane (PDMS) channels suggests that glia, astrocytes, and neural progenitor cells in the culture might also prefer growing into small spaces.[49] However, adding glia would potentially compromise the stated goal of the current study to determine if the tubes can be used to isolate neural axon growth. Further investigation is needed to determine the role of glial cells in supporting long-term neural culture and network formation, as well as to understand the potential in using these materials in *in vivo* applications.

## CONCLUSION

We have demonstrated that the Si/SiGe bilayer nanomembrane is a viable substrate for neural culture. We can make a variety of rolled-up microtubes through strain engineering and standard semiconductor fabrication techniques. The dimensions (length and diameter) and the wall thickness of these structures can all be precisely controlled. The fabrication process does not leave any hazardous residues that affect cell survival. *In vitro* experimentation suggests that primary cortical neurons prefer to grow within and along the tubular topology. Depending on the geometry details, different growth patterns can occur. Selective seeding by PDL printing can be used to assist the positioning of neurons at specific locations, resulting in single-axon outgrowth through the semiconductor tubes. Arrays of such tubes may be used to guide neurites to form predefined neuronal networks. Moreover, with proper diameter size, these tubes might provide a confined 3D contact to the neurite membrane, potentially mimicking the myelin sheath and resulting in improved electrical properties for signal propagation along the neural processes. Micrometer-sized cuff electrodes can easily be made with metal contacts on the inner surface that conform to the tubular structure. In fact, because the substrates are made of semiconductor materials, whose fabrication is well understood and compatible to processes used in the semiconductor industry, it would be possible to add electrical functionality to the tubes for stimulation and probing, making it an integrated platform for cell culture and physiological measurement. Lastly, the tube surface can be coated with polymers, such as parylene. This further increases the surface resistance and decreases the surface capacitance, both of which are beneficial to neuronal signaling. Such a unique platform has great potential for neural-electronic applications.

## METHODS

**Fabrication of Semiconductor Nanomembrane Tubes.** Both optical and electron-beam lithography can be used for patterning. Specific tube features depend on the pattern design and its alignment with respect to the crystallographic direction: a rhombus pattern with its diagonal aligned in the ⟨100⟩ direction results in tubes with tapered ends (Figure 2a), while a rectangular pattern with one edge aligned along ⟨100⟩ provides blunt-ended tubes (Figure 2c). Reactive-ion etching (Unaxis 790) is used to define the patterned areas while exposing the sacrificial layers underneath. We use a mixture of $SF_6$ and $O_2$ gas at 15 mTorr pressure and with 100 W of power. The etching time is 40 s. Vapor-phase HF etching is chosen to remove the $SiO_2$ sacrificial layer. Specifically, we use $HF/H_2O$ (2:1) to etch the structure at 53 °C. The estimated etching speed is about 1 $\mu$m/min. Therefore, by controlling the etching time, we can control the number of turns, hence the wall thickness, for the tube.

**Preculture Treatment.** After HF etching, the substrate containing Si/SiGe tubes is kept in the chemical hood for 2−3 h to ensure the residual HF vapor is fully vented. The substrate is subsequently stored in 70% ethyl alcohol for cleaning and sterilizing. Before coating with poly-D-lysine (PDL), the sterilized substrate is carefully flooded by preautoclaved double-distilled water three times to ensure alcohol is thoroughly rinsed. Starting from this step, every procedure is carried out in a sterile environment.

**PDL Coating and Printing.** Poly-D-lysine in a final concentration of 0.1 mg/mL is coated or printed to facilitate the uniform or selective adhesion during the cell seeding process. A Diamatix Materials Printer (DMP-2800 series, FUJIFILM) is used to deposit a mixture of PDL and fluorescein solution (for inspection) in droplets that are 5−10 $\mu$m in diameter near the inlet of the tubes.

**Neural Culturing.** All of the cell cultures reported in this paper use E15.5 cortical neurons obtained from Swiss Webster mice. The cells are dissociated by treating with trypsin (0.25%, 15 min, 37 °C), then triturated with a micropipet tip, diluted in plating medium (neurobasal medium with 5% FBS, Hyclone, B27 supplement, 2 mM glutamine, 37.5 mM NaCl, and 0.3% glucose) and plated onto the substrates at low density (3000−10 000 cells/cm$^2$). After 1 h, the sample is flooded with serum-free medium (plating medium without FBS) and incubated for 5−7 days. For fluorescent live imaging, the cells are transfected with GFP-α-tubulin (human) in a pCAX vector. Briefly, neurons are resuspended in nucleofector solution (mouse neuron kit, Lonza Walkersville Inc.) and transfected *via* nucleofection in accordance with the manufacturer's directions.

**Sample Preparation for SEM Imaging.** Prior to SEM imaging, the cell culture is fixed in mixed primary fixative of 2% paraformaldehyde/Krebs/sucrose and 2.5% glutaraldehyde in phosphate buffer at pH 7.4 for 30 min, then rinsed three times with phosphate buffered saline (PBS) solution. The cell culture is subsequently treated with postfixative of 1% osmium tetraoxide in phosphate buffer at pH 7.4 for 1 h, and then rinsed thoroughly with PBS solution. A scanning electron microscope (LEO Gemini 1530) is used for SEM imaging.

**Immunostaining and Fluorescent Imaging.** The culture sample for fluorescent imaging is fixed in 4% paraformaldehyde/Krebs/sucrose fixative at pH 7.4 for 30 min. Cultures are then blocked with 10% BSA/PBS, permeabilized in 0.2% Trition X-100/PBS, and labeled with antibodies to tyrosinated tubulin at 1:1000 (YL1/2 clone, Chemicon) and MAP2 at 1:1000 (HM-2 clone, Sigma-Aldrich). Secondary antibodies coupled to Alexa 568 and 647 (Invitrogen) are used at 1:500, and Alexa 488/phalloidin (Invitrogen) is used to label actin filaments (1:100). Both live and

fixed cell cultures are imaged with a Fluoview500 AX70 upright (Olympus, USA) microscope through a 40× water-immersion lens of numerical aperture 0.8.

*Acknowledgment.* We thank M. A. Eriksson and C. Staii for their insights early in this study. M.Y. is supported by NSF/MRSEC (Grant No. DMR-0520527). Y.H. and J.C.W. are supported by NIH (Grant No. NIBIB 1R01EB009103-01). J.B. and E.W.D. acknowledge financial support from the Dana Foundation, the Whitehall Foundation, and NIH (Grant No. NS064014). Sample preparation was supported by AFOSR/MURI (Grant No. FA9550-08-1-0337).

## REFERENCES AND NOTES

1. Weibel, D. B.; Garstecki, P.; Whitesides, G. M. Combining Microscience and Neurobiology. *Curr. Opin. Neurobiol.* **2005,** *15*, 560–567.
2. Pearce, T. M.; Williams, J. C. Microtechnology: Meet Neurobiology. *Lab Chip* **2007,** *7*, 30–40.
3. Vansteensel, M. J.; Hermes, D.; Aarnoutse, E. J.; Bleichner, M. G.; Schalk, G.; van Rijen, P. C.; Leijten, F. S.; Ramsey, N. F. Brain−Computer Interfacing Based on Cognitive Control. *Ann. Neurol.* **2010,** *67*, 809–816.
4. Taylor, D. M.; Tillery, S. H.; Schwartz, A. B. Direct Cortical Control of 3D Neuroprosthetic Devices. *Science* **2002,** *7*, 1829–1832.
5. Merrill, D. R.; Bikson, M.; Jefferys, J. Electrical Stimulation of Excitable Tissue: Design of Efficacious and Safe Protocols. *J. Neurosci. Methods* **2005,** *141*, 171–198.
6. Rutten, W. L. Selective Electrical Interfaces with the Nervous System. *Annu. Rev. Biomed. Eng.* **2002,** *4*, 407–452.
7. Kotov, N. A.; Winter, J. O.; Clements, I. P.; Jan, E.; Timko, B. P.; Campidelli, S.; Pathak, S.; Mazzatenta, A.; Lieber, C. M.; Prato, M.; *et al.* Nanomaterials for Neural Interfaces. *Adv. Mater.* **2009,** *21*, 3970–4004.
8. Pearce, T. M.; Wilson, J. A.; Oakes, S. G.; Chiu, S.; Williams, J. C. Integrated Microelectrode Array and Microfluidics for Temperature Clamp of Sensory Neurons in Culture. *Lab Chip* **2005,** *5*, 97–101.
9. Greve, F.; Frerker, S.; Bittermann, A. G.; Burkhardt, C.; Hierlemann, A.; Hall, H. Molecular Design and Characterization of the Neuron−Microelectrode Array Interface. *Biomaterials* **2007,** *28*, 5246–5258.
10. Patolsky, F.; Timko, B. P.; Yu, G.; Fang, Y.; Greytak, A. B.; Zheng, G.; Lieber, C. M. Detection, Stimulation, and Inhibition of Neuronal Signals with High-Density Nanowire Transistor Arrays. *Science* **2006,** *313*, 1100–1104.
11. Kam, L.; Shain, W.; Turner, J. N.; Bizio, R. Axonal Outgrowth of Hippocampal Neurons on Micro-Scale Networks of Polylysine-Conjugated Laminin. *Biomaterials* **2001,** *22*, 1049–1054.
12. Chang, J. C.; Brewer, G. J.; Wheeler, B. C. A Modified Microstamping Technique Enhances Polylysine Transfer and Neuronal Cell Patterning. *Biomaterials* **2003,** *24*, 2863–2870.
13. Zeck, G.; Fromherz, P. Noninvasive Neuroelectronic Interfacing with Synaptically Connected Snail Neurons Immobilized on a Semiconductor Chip. *Proc. Natl. Acad. Sci. U.S.A.* **2001,** *98*, 10457–10462.
14. Tooker, A.; Meng, E.; Erickson, J.; Tai, Y.; Pine, J. Biocompatible Parylene Neurocages. *IEEE Eng. Med. Biol. Mag.* **2005,** *24*, 30–33.
15. Taylor, A. M.; Blurton-Jones, M.; Rhee, S. W.; Cribbs, D. H.; Cotman, C. W.; Jeon, N. L. A Microfluidic Culture Platform for CNS Axonal Injury, Regeneration and Transport. *Nat. Methods* **2005,** *2*, 599–605.
16. Compston, A.; Zajicek, J.; Sussman, J.; Webb, A.; Hall, G.; Muir, D.; Shaw, C.; Wood, A. Scolding, N. Review: Glial Lineages and Myelination in the Central Nervous System. *J. Anat.* **1997,** *190*, 161–200.
17. Sherman, D. L.; Brophy, P. J. Mechanisms of Axon Ensheathment and Myelin Growth. *Nat. Rev. Neurosci.* **2005,** *6*, 683–690.
18. Funch, P. G.; Faber, D. S. Measurement of Myelin Sheath Resistances: Implications for Axonal Conduction and Pathophysiology. *Science* **1984,** *225*, 538–540.
19. Naples, G. G.; Mortimer, J. T.; Yuen, T. Overview of Peripheral Nerve Electrode Design and Implantation. In *Neural Prostheses: Fundamental Studies, Biophysics and Bioengineering Series*; Agnew, W. F., McCreery, D. B., Eds.; Prentice Hall: New Jersey, 1990; pp 107−144.
20. Prinz, V. Y.; Seleznev, V. A.; Gutakovsky, A. K.; Chehovskiy, A. V.; Preobrazhenskii, V. V.; Putyato, M. A.; Gavrilova, T. A. Free-Standing and Overgrown InGaAs/GaAs Nanotubes, Nanohelices and Their Arrays. *Physica E* **2000,** *6*, 828–831.
21. Schmidt, O. G.; Eberl, K. Nanotechnology: Thin Solid Films Roll up into Nanotubes. *Nature* **2001,** *410*, 168.
22. Qin, H.; Shaji, N.; Merrill, N. E.; Kim, H.; Toonen, R. C.; Blick, R. H.; Roberts, M. M.; Savage, D. E.; Lagally, M. G.; Celler, G. Formation of Microtubes from Strained SiGe/Si Heterostructures. *New J. Phys.* **2005,** *7*, 241−1–10.
23. Golod, S. V.; Prinz, V. Y.; Mashanov, V. I.; Gutakovsky, A. K. Fabrication of Conducting GeSi/Si Micro- and Nanotubes and Helical Microcoils. *Semicond. Sci. Technol.* **2001,** *16*, 181–185.
24. Cavallo, F.; Lagally, M. G. Semiconductor Turn Soft: Inorganic Nanomembranes. *Soft Matter* **2009,** *6*, 439–455.
25. Huang, M.; Cavallo, F.; Liu, F.; Lagally, M. G. Nanomechanical Architecture of Semiconductor Nanomembranes. *Nanoscale* **2011,** *3*, 96–120.
26. Berthold, C. H.; Nilsson, I.; Rydmark, M. Axon Diameter and Myelin Sheath Thickness in Nerve Fibres of the Ventral Spinal Root of the Seventh Lumbar Nerve of the Adult and Developing Cat. *J. Anat.* **1983,** *136*, 483–508.
27. *Bioelectricity: A Quantitative Approach*, 2nd ed.; Plonsey, R., Barr, R. C., Eds; Springer: Berlin, 2000.
28. Kipke, D. R.; Shain, W.; Buzsaki, G.; Fetz, E.; Henderson, J. M.; Hetke, J. F.; Schalk, G. Advanced Neurotechnologies for Chronic Neural Interfaces: New Horizons and Clinical Opportunities. *J. Neurosci.* **2008,** *28*, 11830–11838.
29. Cogan, S. F. Neural Stimulation and Recording Electrodes. *Annu. Rev. Biomed. Eng.* **2008,** *10*, 275–309.
30. Dent, E. W.; Kwiatkowski, A. V.; Mebane, L. M.; Philippar, U.; Barzik, M.; Rubinson, D. A.; Gupton, S.; Van Veen, J. E.; Furman, C.; Zhang, J.; *et al.* Filopodia Are Required for Cortical Neurite Initiation. *Nat. Cell Biol.* **2007,** *9*, 1347–1359.
31. Hu, X.; Viesselmann, C.; Nam, S.; Merriam, E.; Dent, E. W. Activity-Dependent Dynamic Microtubule Invasion of Dendritic Spines. *J. Neurosci.* **2008,** *28*, 13094–13105.
32. Rowe, L.; Almasri, M.; Lee, K.; Fogleman, N.; Brewer, G. J.; Nam, Y.; Wheeler, B. C.; Vukasinovic, J.; Glezer, A.; Frazier, A. B. Active 3-D Microscaffold System with Fluid Perfusion for Culturing *In Vitro* Neuronal Networks. *Lab Chip* **2007,** *7*, 475–482.
33. Huang, G.; Mei, Y.; Thurmer, D. J.; Coric, E.; Schmidt, O. G. Rolled-up Transparent Microtubes as Two-Dimensionally Confined Culture Scaffolds of Individual Yeast Cells. *Lab Chip* **2009,** *9*, 263–268.
34. Schulze, S.; Huang, G.; Krause, M.; Aubyn, D.; Quinones, V. A.; Schmidt, C. K.; Schmidt, O. G. Morphological Differentiation of Neurons on Microtopographic Substrates Fabricated by Rolled-up Nanotechnology. *Adv. Eng. Mater.* **2010,** *12*, B558–B564.
35. Goldner, J. S.; Bruder, J. M.; Li, G.; Gazzola, D.; Hoffman-Kim, D. Neurite Bridging across Micropatterned Grooves. *Biomaterials* **2006,** *27*, 460–472.
36. Scheibel, A. B.; Paul, L.; Fried, I. Scanning Electron Microscopy of the Central Nervous System. I. The Cerebellum. *Brain Res. Rev.* **1981,** *3*, 207–228.
37. Hoffman-Kim, D.; Mitchel, J. A.; Bellamkonda, R. V. Topography, Cell Response, and Nerve Regeneration. *Annu. Rev. Biomed. Eng.* **2010,** *12*, 203–231.
38. Staii, C.; Viesselmann, C.; Ballweg, J.; Shi, L.; Liu, G.; Williams, J. C.; Dent, E. W.; Coppersmith, S. N.; Eriksson, M. A. Positioning and Guidance of Neurons on Gold Surfaces by Directed Assembly of Proteins Using Atomic Force Microscopy. *Biomaterials* **2009,** *30*, 3397–3404.
39. Dotti, C. G.; Sullivan, C. A.; Banker, G. A. The Establishment of Polarity by Hippocampal Neurons in Culture. *J. Neurosci.* **1988,** *8*, 1454–1468.

40. Koch, C. *Biophysics of Computation: Information Processing in Single Neurons*; Oxford University Press: New York, 1998.
41. Blight, A. B. Computer Simulation of Action Potentials and Afterpotentials in Mammalian Myelinated Axons: The Case for a Lower Resistance Myelin Sheath. *Neuroscience* **1985,** *15*, 13–31.
42. Delivopoulos, E.; Murray, A. F.; MacLeod, N. K.; Curtis, J. C. Guided Growth of Neurons and Glia Using Microfabricated Patterns of Parylene-C on a $SiO_2$ Background. *Biomaterials* **2009,** *30*, 2048–2058.
43. Mendach, S.; Schumacher, O.; Welsch, H.; Heyn, C.; Hansen, W. Evenly Curved Two-Dimensional Electron Systems in Rolled-up Hall Bars. *Appl. Phys. Lett.* **2006,** *88*, 212113.
44. Ackermann, D. M.; Bhadra, N.; Foldes, E. L.; Wang, X.; Kilgore, K. L. Effect of Nerve Cuff Electrode Geometry on Onset Response Firing in High-Frequency Nerve Conduction Block. *IEEE Trans. Neural Syst. Rehabil. Eng.* **2010,** *18*, 658–665.
45. Schiefer, M. A.; Polasek, K. H.; Triolo, R. J.; Pinault, G. C.; Tyler, D. J. Selective Stimulation of the Human Femoral Nerve with a Flat Interface Nerve Electrode. *J. Neural Eng.* **2010,** *7*, 026006.
46. Navarro, X.; Krueger, T. B.; Lago, N.; Micera, S.; Stieglitz, T.; Dario, P. A Critical Review of Interfaces with the Peripheral Nervous System for the Control of Neuroprostheses and Hybrid Ionic Systems. *J. Peripher. Nerv. Syst.* **2005,** *10*, 229–258.
47. Polikov, V. S.; Block, M. L.; Fellous, J.; Hong, J.; Reichert, W. M. *In Vitro* Model of Glial Scarring around Neuroelectrodes Chronically Implanted in the CNS. *Biomaterials* **2006,** *27*, 5368–5376.
48. Nam, Y.; Chang, J.; Khatami, D.; Brewer, G. J.; Wheeler, B. C. Patterning to Enhance Activity of Cultured Neuronal Networks. *IEE Proc. Nanobiotechnol.* **2004,** *151*, 109–115.
49. Huang, Y.; Agrawal, B.; Sun, D.; Kuo, J. S.; Williams, J. C. Microfluidics-Based Devices: New Tools for Studying Cancer and Cancer Stem Cell Migration. *Biomicrofluidics* **2011**, DOI:10.1063/1.3555195.